AIAA 82-4284

Blunt Fin-Induced Shock Wave/Turbulent Boundary-Layer Interaction

D.S. Dolling* and S.M. Bogdonoff†
Princeton University, Princeton, New Jersey

This paper presents results from an experimental study of blunt fin-induced shock wave/turbulent boundary-layer interaction. Semi-infinite fin models with hemicylindrical, unswept leading edges were tested in Mach 3, high Reynolds number, turbulent boundary layers. All tests were made under approximately adiabatic wall conditions. The program had two fundamental objectives. The first was to examine the spanwise development of the disturbed flowfield and to determine its dependence on the configuration geometry and incoming flow conditions. To achieve this, streamwise surface pressure distributions were measured in the region extending from the centerline to 110 fin diameters outboard. The second objective was to determine the vertical extent of the interaction on the fin. This was carried out using a fin model whose leading edge and side face were instrumented with pressure taps. The results show that, on the test surface near the fin and on the fin itself, the leading-edge diameter plays a dominant role in determining the interaction's scale and characteristics.

Introduction

THE disturbed flowfield induced by a hemicylindrically blunted fin (or circular cylinder) in a supersonic turbulent boundary layer has been studied by many investigators over the last 30 years. It is an extremely difficult problem. The flowfield is dominated by a three-dimensional (3-D), highly unsteady shock wave structure generating complex distributions of surface properties with steep streamwise and spanwise gradients. Very high pressures and heat-transfer rates occur on the fin and on the surface near the root. The practical need to predict these has provided much of the driving force behind such sustained interest in the problem.

In a general sense, this interaction is a member of a class of flows in which a skewed shock wave interacts with a turbulent boundary layer. Such interactions occur in many practical situations, ranging from the planar shock-induced flowfield on the sidewalls of engine inlets to the classic blunt fin/body junction problem being studied here. Certain of these flows, such as the planar skewed shock interaction, can now be simulated numerically,[1-3] but as far as is known, no codes exist that are capable of predicting the blunt fin-induced flowfield. The current, limited knowledge of this interaction is based entirely on experiment.

A schematic illustrating the general problem is shown in Fig. 1. It involves many parameters. Geometrically these include fin height h, leading-edge diameter D, sweep angle Λ, and angle of attack α. The incoming flow is characterized by its Mach number M_∞, Reynolds number Re_∞, and the properties of the boundary layer. In the current study, only unswept ($\Lambda = 0$ deg), semi-infinite fins were tested. Semi-infinite means that the "asymptotic result" is produced, a condition occurring when further increases in h do not alter the disturbed flowfield. In the past there has been confusion over the conditions under which this will occur. The situation is clarified in Ref. 4, where it is shown that the physically relevant parameter is h/D, not h/δ.

There exists a large body of references dealing with various aspects of these interactions. It is far too extensive to review thoroughly here. A survey article on the effects of small protuberances on boundary-layer flows complied by Sedney[5] contains a bibliography of the relevant work prior to 1973. Small protuberances are defined as being those for which h/δ is 0[1] or less and whose effect on the external flowfield is small. This definition can be contradictory, since a body classified by it as being small may generate the "asymptotic result."[4] In an earlier review article, Korkegi[6] summarized results from blunt fin experiments carried out before 1971. These mainly involved semi-infinite fins. A more recent critical review, also for semi-infinite cases, was compiled by Cosad.[7]

In many studies, the major objective was to determine the centerline and fin (or cylinder) leading-edge characteristics. Much of the data consist of surface pressure distributions and oil streak patterns. Tests have been made over a fairly wide range of conditions to determine the dependence of the interaction properties on D,[8-17] Λ,[10,18,19] h,[8,10,13] δ,[8,12,14-17] M_∞,[8,10,11,15] and Re_∞.[8,10,15,18,19] Attempts have been made to correlate the data, but confusion over the conditions necessary for a model to be considered semi-infinite has caused some difficulty, particularly with respect to the vertical scale of the flowfield. Although contradictory evidence exists concerning the effects of some parameters, such as M_∞, the experiments showed clearly that the dominant parameters controlling the centerline flowfield are D and Λ.

The development of the flowfield in the spanwise direction, Y, has received little attention. If detailed distributions of

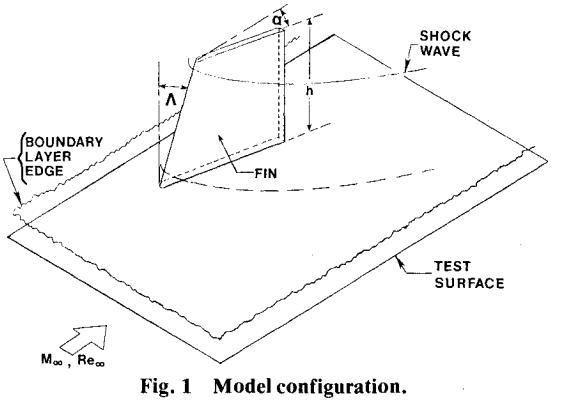

Fig. 1 Model configuration.

Received Sept. 23, 1981; revision received April 12, 1982.

*Research Staff Member and Lecturer, Dept. of Mechanical and Aerospace Engineering. Member AIAA.

†Professor and Chairman, Dept. of Mechanical and Aerospace Engineering. Fellow AIAA.

surface properties are to be measured, extensive instrumentation is required, and even a very limited parametric study is time-consuming and very expensive. One of the most extensive studies to date is that of Ref. 10. Wall pressure distributions were measured at spanwise stations for a wide range of D, Λ, and h at several values of M_∞ and Re_∞. The dominant roles of D and Λ are clearly seen. However, correlations of the spanwise results are not presented. Sedney[8], Westkaemper,[13] and Winkelmann[18] have also made detailed investigations, but the main focus of these was on the flowfield scale and properties on and near the centerline.

The major objective of the present study was to examine the spanwise development of the interaction. Tests were made using different-diameter fins in several high Reynolds number, Mach 3, turbulent boundary layers. Streamwise surface pressure distributions were measured for $0 \le \alpha \le 12$ deg over the region defined by $0 \le Y/D \le 110$. The aim of such extensive testing was to determine not only the spanwise development of the interaction but also the key parameters controlling the scales and characteristics. The second objective of the study was to examine the vertical extent of the disturbed flowfield and to clarify the role that δ has in controlling the leading-edge characteristics. To do this, an instrumented fin model was tested in several different turbulent boundary layers. Results of these experiments are presented in this paper.

Experimental Program

Wind Tunnel and Models

The experiments were carried out in the Princeton University 20 cm × 20 cm (8 in. × 8 in.) high Reynolds number, supersonic blowdown tunnel. This facility operates at a nominal freestream Mach number of 3 and at stagnation pressures in the range 4×10^5 to 3.4×10^6 Nm^{-2} (60-500 psia).

The model geometry is shown in Fig. 1. The coordinate system used in the description below and for data presentation is shown in Fig. 2. Two instrumented test surfaces were used: the tunnel floor and a horizontal flat plate with a sharp leading edge that spanned the tunnel. On both surfaces the fins could be positioned at various streamwise locations. Both surfaces were instrumented with several rows of pressure tappings aligned with the X axis. The tappings were 0.102 cm (0.040 in.) in diameter with a minimum streamwise spacing of 0.25 cm (0.1 in.).

The tests were made in two series. In the first series, the fin was supported by bearings near the leading edge and held by an arm attached to its rear face. The arm passed through the tunnel sidewall to a drive mechanism that allowed the angle of attack to be changed during a test. It could be varied in the range 0-12 deg. Nylon seals at the floor and ceiling junctions prevented leakage. Eight fins were used, with D in the range of 0.102 to 1.27 cm (0.040 to 0.5 in.). They were all 25 cm (10 in.) long. In the second test series, the fin was fixed at zero angle of attack and held at the rear by an axial sting. Fins with

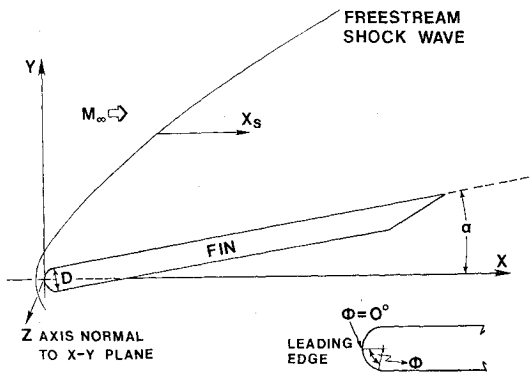

Fig. 2 Coordinate system.

D in the range 0.165 to 2.54 cm (0.065 to 1.0 in.) were tested. A fin/sting adapter permitted lateral translation of the model relative to the fixed rows of pressure taps, allowing streamwise pressure distributions to be measured anywhere in the range $0 \le Y/D \le 4$. One fin [$D = 1.27$ cm (0.5 in.)] was instrumented with six vertical rows of pressure taps. Three rows were on the leading edge at $\phi = 0$, 45, and 90 deg, respectively (Fig. 2). The other three were on the side face at $X = 3.18$, 5.71, and 8.26 cm (1.25, 2.25, and 3.25 in.), respectively. Two nylon seals of thickness 0.13 and 0.25 cm (0.05 and 0.1 in.) that could be used interchangeably served the dual purpose of sealing the fin base/tunnel floor interface and doubling the pressure tapping density.

Test Conditions and Incoming Boundary Layers

Most tests were made at a stagnation pressure of 6.8×10^5 Nm^{-2} (100 psia). The stagnation temperature was 260 K ± 5%, and the model wall temperature was approximately adiabatic. These flow conditions resulted in a freestream unit Reynolds number Re_∞ of 6.5×10^7 m^{-1} ±5%.

Depending on streamwise position, the undisturbed boundary-layer thickness at the location of the fin leading edge varied from 1.24 to 2.03 cm (0.49 to 0.8 in.) on the tunnel floor and from 0.13 to 0.33 cm (0.05 to 0.13 in.) on the flat plate. Boundary-layer trips were not used. On the flat plate, natural transition occurred within about 2 cm (0.8 in.) of the leading edge. The undisturbed boundary-layer development on both test surfaces has been measured. Both boundary layers are in equilibrium, two-dimensional, and fully turbulent. Their mean velocity profiles match the well known wall-wake similarity law.

Shock Wave Shapes

For comparing data from different interactions, it is essential that the freestream shock wave position be known accurately, since it is used as a reference location throughout the flowfield. A set of variable diameter, sting mounted fins was tested in the tunnel freestream, and shadow photographs were taken of the shock waves. From these, plots of shock wave shape as a function of D and α were obtained.[16]

Discussion of Results

The results show that the flowfield can be split into three regions: an "inner" one, an "outer" one, and a "boundary" zone between them. In each region, different parameters control the scale and properties. In the outer region, these parameters are the same as in planar skewed shock wave interactions. This means that, at a certain spanwise station in the blunt fin flowfield, the properties are the same as if the leading edge were sharp. Outboard of this station, blunt and sharp fin-induced interactions develop in the same way.

The boundary between the inner and outer regions cannot be defined precisely, since the two zones merge gradually. This merging process is complex and is the subject of a separate paper.[20] It is shown there that the boundary position depends primarily on D and α. The current paper is restricted to a discussion of the interaction properties in the inner region of the flowfield.

Centerline Scale and Characteristics

Microsecond spark schlieren and shadow photographs of the flowfield upstream of the fin leading edge show that the region near the root is characterized by a highly unsteady shock wave structure. Four photographs, taken at random intervals, are shown in Fig. 3. Several series of photographs taken using a Dynafax camera[21] at a framing rate of 35 kHz and with an exposure time of 0.75 μs showed no evidence of periodic motion. Tests using high-frequency response pressure transducers showed that large-amplitude surface pressure fluctuations occur with rms levels up to two orders of magnitude higher than at the wall under the incoming

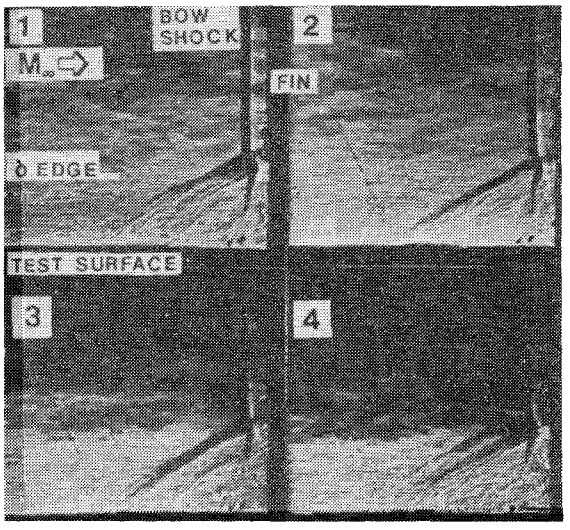

Fig. 3 Shock wave structures upstream of fin leading edge.

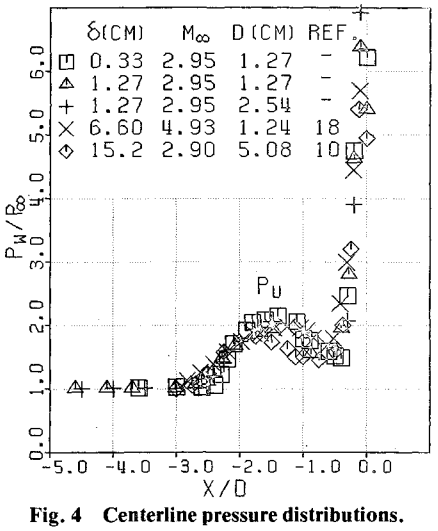

Fig. 4 Centerline pressure distributions.

boundary layer.[22] The spectra showed that the energy distribution was broadband. The unsteadiness of the wave structure decays fairly rapidly in the spanwise direction and is confined mainly to the region upstream of the freestream shock wave.

The mean surface pressure distribution on centerline is similar in shape to that upstream of a 2-D forward-facing step. Distributions from the present study and two others are shown in Fig. 4. The tests were made at $\alpha = 0$ deg. The wall pressure P_w is normalized by the undisturbed freestream static value P_∞ and the streamwise distance X is normalized by D. In these flows δ varied by about 46:1 and D varied by 4:1. For the thickest boundary layer, shadowgraphs[10] showed that the root shock wave structure was buried within the boundary layer approaching the leading edge. With the thinnest boundary layer, the wave structure was predominantly outside it. Over this range, normalizing X by D correlates to first order both the upstream influence, Lu, and the locations of the characteristic features of the pressure distributions. The boundary-layer thickness does not play a primary role in controlling the interaction scale. Lu varies from about 1 to 11 δ, whereas, in terms of D, it falls in the narrow range of about 2.7 to 3D.

In addition to the length scale being determined primarily by D, the details of the pressure distribution are relatively insensitive to changes in flow parameters. Price and Stallings' data[10] at fixed Re_∞ but variable M_∞ showed a small increase

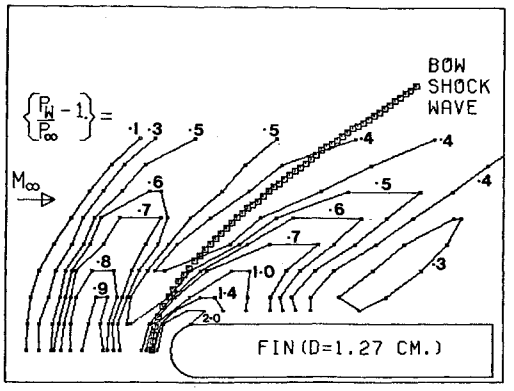

Fig. 5 Surface pressure contours ($0 \le Y/D \le 4$) for $\alpha = 0$ deg.

in P_w/P_∞ from 1.75 to about 2.0 at the upstream peak P_u as M_∞ was increased from 2.30 to 4.44. There was no measurable effect on Lu. Winkelmann's data[18] at $M_\infty = 4.93$, also shown in Fig. 4, correlate well with the Mach 3 results, indicating that M_∞ does not play a critical role in controlling the centerline characteristics. Tests at fixed M_∞ but variable Re_∞, also from Ref. 10, showed that changes in Re_∞ have only small effects on Lu and overall pressure levels.

The present data show a consistent, but weak, decrease in Lu/D with increasing D/δ. Careful examination of other data sets shows the same trend. In Ref. 4 it was shown that the present data set and 11 others could be correlated reasonably well by plotting Lu/D as a function of D/δ. These data spanned the range $2.2 \le M_\infty \le 5$, 0.33 cm $\le \delta \le$ 15 cm. For small D/δ ($< \sim 1$), Lu was about 3D, decreasing to about 2D at D/δ around 7 to 10. This range of D/δ includes flows in which the root shock wave structure was fully immersed in, partially immersed in, or predominantly outside the boundary layer. As Lu/D decreases with increasing D/δ, the pressure ratio at the upstream peak P_u increases. The present tests show that this pressure ratio reaches an approximately constant value when D/δ reaches a level such that the root shock wave structure is predominantly outside the boundary layer.

Recent measurements by Hung and Clauss[23] at $M_\infty = 5.3$ show that Lu depends critically on the state of the incoming boundary layer. In the laminar case, Lu was observed to be of the order of 9 to 12D, a fourfold increase over the turbulent case. It also depends on the leading-edge shape. For fixed flow conditions, Lu for a flat-faced fin of thickness t is approximately twice that for a hemicylindrically blunted model with $D = t$ (Ref. 24).

Spanwise Interaction Scaling and Characteristics

The characteristic peaked pressure distribution shown in Fig. 4 also exists off centerline. Detailed streamwise pressure distributions in the range $0 \le Y/D \le 4$ were measured at $\alpha = 0$ deg, and from these a pressure contour map was constructed. It is shown in Fig. 5. The incoming boundary layer was 1.27 cm (0.5 in.) thick. The downstream pressure peak, which on centerline has $P_w/P_\infty \sim 6$, decays rapidly with spanwise distance. At $Y/D = 1$ it has dropped to about 2, and by $Y/D = 5$ it is barely detectable. Further outboard, the pressure distribution is characterized by a single peak, which decays gradually; at $Y/D = 55$, $P_w/P_\infty \sim 1.1$. The streamwise length scale of the interaction increases spanwise and results mainly from an increase in upstream influence. Downstream of the freestream shock wave the streamwise length scale is approximately constant. At $X_s/D \sim +5$, in the region near the fin, P_w reaches a common level that decreases streamwise at a rate independent of Y/D.

The present tests show that the interaction scale in this inner region is dependent primarily on D. In this sense, the flowfield can be considered as being "leading-edge

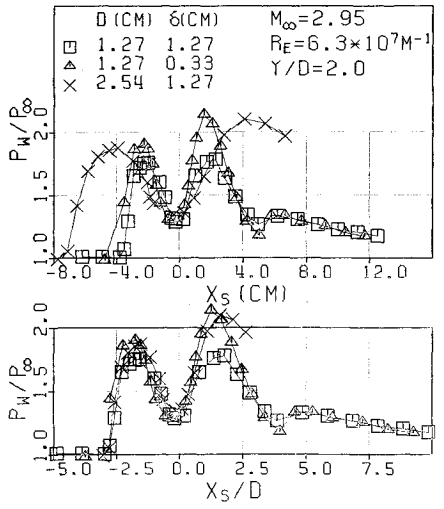

Fig. 6 Use of D as an interaction scaling parameter ($Y/D = 2$).

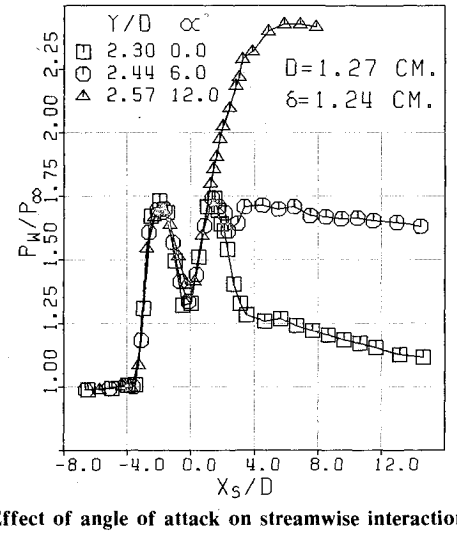

Fig. 7 Effect of angle of attack on streamwise interaction pressure distribution.

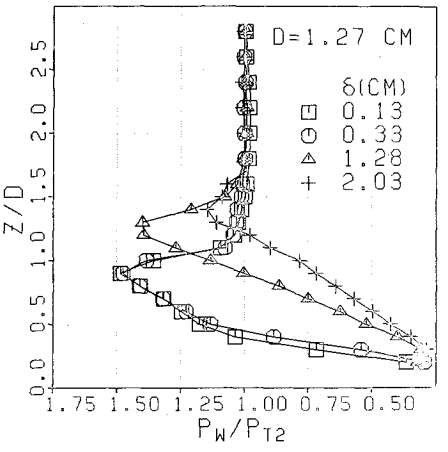

Fig. 8 Effect of incoming boundary-layer thickness on fin leading-edge pressure distributions.

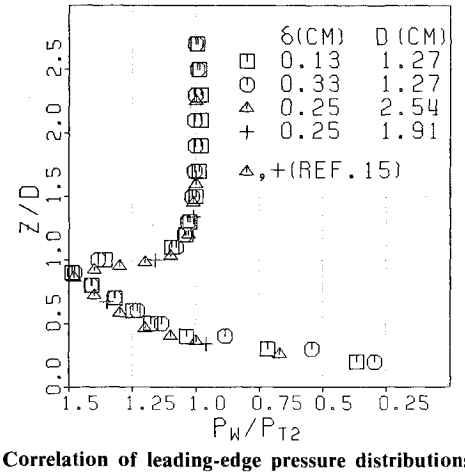

Fig. 9 Correlation of leading-edge pressure distributions for large D/δ.

dominated." Data from interactions generated by different fins in different boundary layers can be correlated if both X_s and Y are normalized by D. Figure 6 shows this for three streamwise pressure distributions at $Y/D = 2$, $\alpha = 0$ deg. In the upper half of the figure, in the plot vs X_s, varying δ with D fixed has little effect on the interaction scale, whereas varying D with δ with fixed alters it substantially. Normalizing X_s by D, as in the lower half of the figure, correlates the interaction scale. Similar to the centerline behavior, both Lu/D and the pressure ratio at the peaks are weak functions of D/δ (Ref. 24). This correlation technique was checked over a wide range of conditions and worked well for all angles of attack tested.

The spanwise extent of this leading-edge-dominated region defines the boundary between the inner and outer zones. The approximate location of this boundary can be specified in terms of Y/D and is a function of α. Under the present test conditions, it varies from $Y/D \sim 8$ at $\alpha = 12$ deg to $Y/D \sim 30$ at $\alpha = 4$ deg. The reasons are connected with the angle-of-attack characteristics of the shock wave shape and are discussed in Ref. 20.

The effect of α on the pressure distribution depends strongly on position Y/D. At $\alpha = 0$ deg, the local shock wave angle β decreases rapidly from 90 deg on centerline to about 35 deg at $Y/D = 5$. It then decreases gradually to 25 deg at $Y/D \sim 25$. For $0 \leq Y/D \leq 5 \sim 6$, β is essentially independent of α over the range 0-12 deg. This means that in this region the shock wave orientation in the flowfield is fixed. Under these conditions, as shown in Fig. 7, a change in α has little effect on the upstream part of the pressure distribution, although it does, of course, affect the final pressure ratio. At larger values of Y/D, β depends on α, and this dependence affects the details of the initial pressure rise as well as the final pressure ratio. However, there is little effect on upstream influence or overall interaction length scale. This very weak dependence of upstream influence on shock wave strength is a characteristic property of both sharp[25] and blunt fin-induced interactions.

Fin Pressure Distributions

The instrumented fin model was tested in four different incoming boundary layers. Leading-edge ($\phi = 0$ deg) pressure distributions are shown in Fig. 8. The surface pressure is normalized by the freestream pitot pressure Pt_2 and the distance Z from the root is normalized by D. For these four flows, D is fixed but has been used to normalize Z since, as will be shown below, it is the appropriate scaling parameter for the vertical extent of the disturbed flow. In these four cases, the root shock wave structure is isolated from the free end by a 2-D central region in which $P_w = Pt_2$. Under these conditions, the asymptotic result occurs and the fin is effectively semi-infinite.

The interaction between the centerline oblique shock wave and the fin bow shock, designated Type IV by Edney,[26] results in the formation of a supersonic jet embedded in a subsonic region. Stagnation pressure losses through the oblique shock wave structure of this jet are small, and pressures in excess of Pt_2 occur at the impact point on the fin.

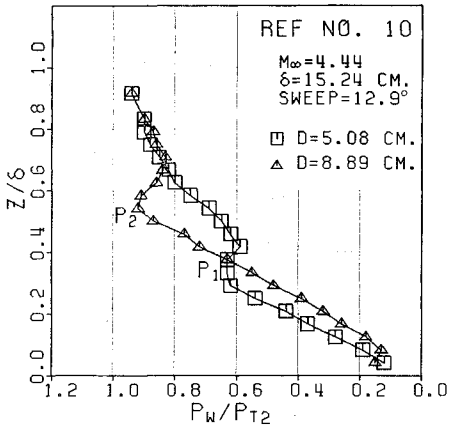

Fig. 10 Price and Stallings' fin leading-edge pressure distribution.[10]

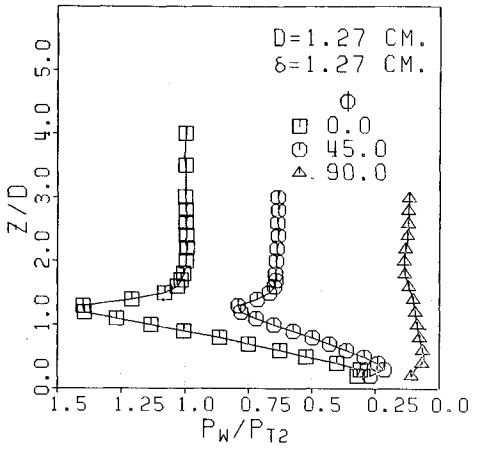

Fig. 12 Pressure distributions around the fin leading edge.

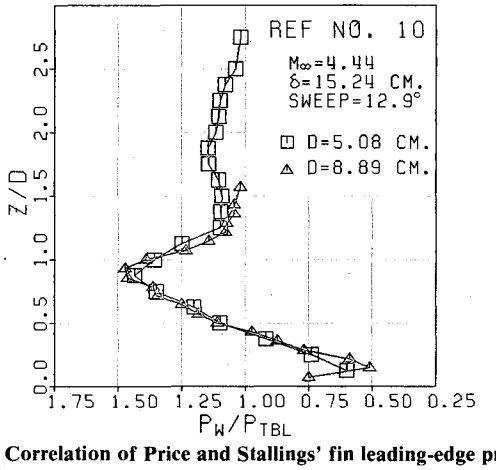

Fig. 11 Correlation of Price and Stallings' fin leading-edge pressure distribution.

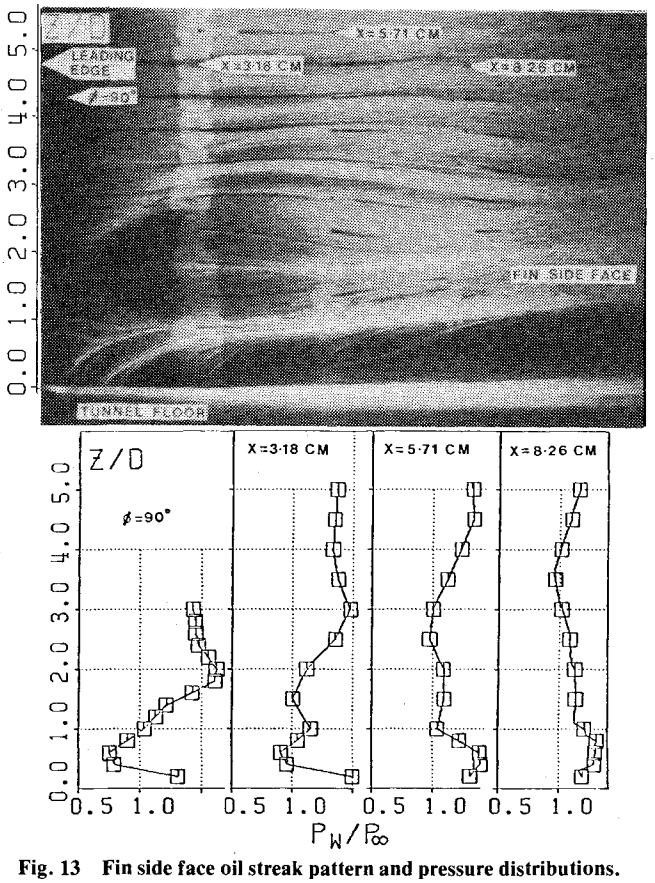

Fig. 13 Fin side face oil streak pattern and pressure distributions.

The ratio of impact pressure to Pt_2 depends on M_∞ and on the flow deflection angle through the oblique shock wave. It can be calculated using inviscid analysis.[26] For the present flow conditions, the impact pressure is about $1.5Pt_2$ or less. At hypersonic speed, it may be an order of magnitude or more higher.

If Lu/δ is large, which is the case if D/δ is large (since $Lu \sim 2$ to $3D$), then the shock wave structure and the jet are predominantly outside the boundary layer. This is true for the two thinner boundary-layer flows in Fig. 8. For these two, $D/\delta \sim 4$ and 10 and $Lu/\delta \sim 11$ and 28, respectively. Under these conditions, the jet impact position and leading-edge pressure distribution in different interactions can be correlated if Z is normalized by D. Figure 9 shows the current data together with measurements made by Kaufmann et al.[15] using larger-diameter fins. They are all at the same M_∞. The locations of the characteristic features of the pressure distribution all correlate on D. In each case, a fin height of about $2D$ would be sufficient for it to be considered semi-infinite.

When D/δ is small, the root shock wave structure still exists, but is either partially or fully submerged in the boundary layer. The basic features of the leading-edge pressure distribution are unaltered, although the impact position of the jet and its pressure ratio are modified, since the shock wave structure occurs in a nonuniform incoming flow. In the present tests, the jet impact position moves up and the peak pressure ratio decreases as the wave structure is progressively immersed in the boundary layer (Fig. 8). Although changes in δ modify the details of leading-edge properties, the basic physical scale is still controlled primarily by D.

For different diameter fins in the same thick boundary layer, this dependence on D and local incoming conditions can be seen using data from Ref. 10. Leading-edge ($\phi = 0$ deg) pressures were measured on different diameter, sweptback fins at $M_\infty = 4.44$. The boundary layer was 15 cm thick. Figure 10 shows these data plotted in their original form as a function of Z/δ. P_1 and P_2 are the jet impact pressures, which are low because of immersion in the boundary layer. P_2 is larger than P_1 since the jet is formed higher up in the layer, where the local pitot pressure and Mach number are higher. The peaks occur at different values of Z/δ, namely, 0.33 and 0.58. Both of these values correspond to Z/D of approximately one. Thus, normalizing Z by D will correlate the peak pressure locations. Further, as shown in Fig. 11, if the surface pressure at a given Z is normalized by the pitot pressure Pt_{BL} at the same Z in the incoming boundary layer, then the pressure distributions correlate.

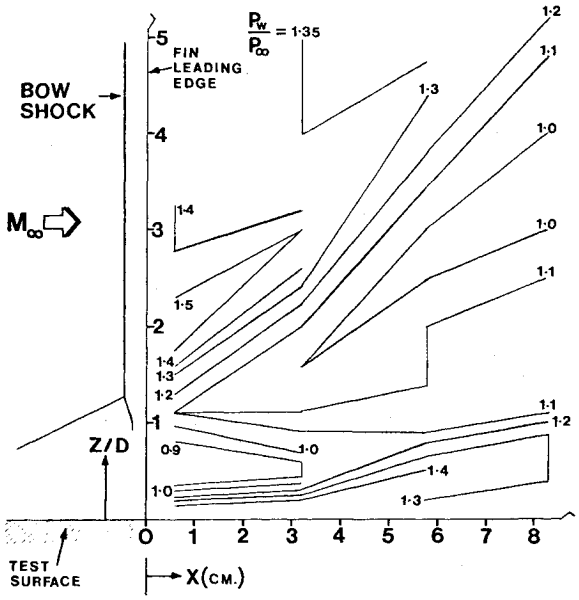

Fig. 14 Fin side face pressure contours.

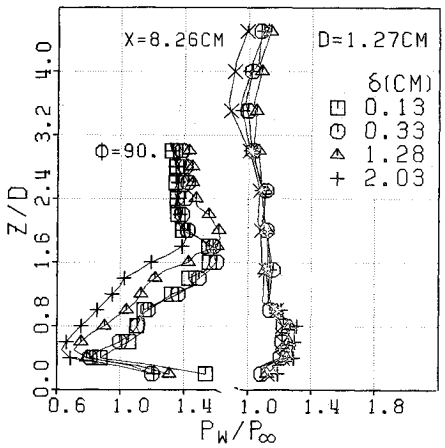

Fig. 15 Effect of boundary-layer thickness on fin side face pressure distributions.

In the present tests, leading-edge pressures were also measured at $\phi = 45$ and 90 deg. One set of results, for $\delta = 1.27$ cm, are shown in Fig. 12; the other three have the same characteristics. Over the central region, P_w/Pt_2 decreases from 1 at $\phi = 0$ deg to 0.64 at $\phi = 45$ deg. This agrees well with measurements of Tewfik and Giedt.[27] At $\phi = 45$ deg the pressure distribution retains the same shape as at $\phi = 0$ deg. The peak is well defined and is at the same vertical position. Depending on the incoming conditions, its pressure level is about 55-58% of that at $\phi = 0$ deg. At $\phi = 90$ deg, the peak is no longer detectable and the pressure distribution, in the form P_w/Pt_2 is fairly uniform. Qualitatively these results are similar to those of Miller[28] at $M_\infty = 4.88$.

Figure 13 shows a surface oil streak pattern on the side face of the fin. δ is 1.27 cm. The leading edge is swept almost clean, although some streaks can be seen between pressure taps at $\phi = 45$ and 90 deg. Wall pressure distributions at $\phi = 90$ deg and at the three downstream rows are shown underneath. From these distributions, constant-pressure contours were constructed. They are shown in Fig. 14. The contour plots for the other three incoming boundary layers have the same characteristics. In the region of the root and for several diameters downstream of the leading edge, a complex streak pattern exists that is reflected in the features of the pressure distributions.

From $\phi = 45$ to 90 deg, the streak lines are parallel to the X axis for $Z > \sim 2D$. In this region the pressures are the same as on an isolated circular cylinder in the same freestream. Below the region of jet impact, the streaks initially flow down and then turn rather sharply and merge with a stream flowing up from the root. At $\phi = 90$ deg, the knee in the pressure distribution occurs where the streaks merge. In contrast, the originally parallel streaks higher up on the fin tend to move upward in the region downstream of $\phi = 90$ deg, causing a bulge in the surface pattern. Although the external flowfield cannot be inferred easily from these surface measurements alone, they do provide clues to the physical nature of the flowfield.

The structure that develops in the corner between the fin and the test surface is relatively insensitive to substantial changes in the incoming boundary-layer thickness. Pressure distributions at $\phi = 90$ deg and the other downstream rows have the same basic shape, and their minima and maxima occur at the same physical locations. Figure 15 shows distributions at $\phi = 90$ deg and at $X = 8.26$ cm for different incoming boundary layers. At $\phi = 90$ deg, the shapes are the same but the levels differ. With increasing X, the distributions at a given station become progressively closer. At $X = 8.26$ cm, they differ by only a few percent. On the leading edge, the scale of the flowfield is controlled primarily by D, with changes in δ producing essentially second-order modifications. Near the leading-edge root, a thicker incoming boundary layer results in lower pressures. Within a short distance downstream, the effects of δ are effectively washed out, even near the root. At $X = 8.26$ cm (3.25 in.), the pressure distribution near the root ($0 \leq Z/D \leq \sim 1$) is essentially independent of δ.

Concluding Remarks

An experimental study has been made of blunt fin-induced shock wave/turbulent boundary-layer interaction. Tests were made in high Reynolds number, Mach 3 boundary layers using semi-infinite fins with hemicylindrical, unswept leading edges. The wall temperature condition was approximately adiabatic. Surface pressure distributions were measured on the flat test surface and on the fin leading edge and side face. The objective of this study was to examine the interaction scaling and characteristics in the region close to the fin and on the fin itself. The measurements have shown that:

1) On centerline, the scale of the disturbed flowfield is controlled primarily by the fin leading-edge diameter D. Upstream influence Lu is typically between 2 and 3D. The pressure distribution is characterized by two peaks whose locations correlate with D. Substantial changes in incoming boundary-layer thickness δ have only second-order effects on the interaction scale and characteristics. These second-order effects, which influence the value of Lu/D and the peak pressure levels, correlate with the parameter D/δ.

2) Off centerline, there exists an "inner" region of the flowfield in which the primary scaling parameter is also D. The spanwise extent of this inner region can be defined in terms of Y/D and is a function of angle of attack. At a common value of Y/D and at a fixed angle of attack, pressure distributions generated using different fins in different boundary layers can be correlated if the distance from the freestream shock wave X_s is normalized by D. The effects of angle of attack on the shape of the pressure distribution depend strongly on spanwise position. At a given station, upstream influence is essentially independent of angle of attack.

3) The fin leading-edge pressure distribution is characterized by a sharp peak caused by impingement of a jet formed in the interaction between the centerline and bow shock waves. For large D/δ, when this shock wave structure is predominantly outside the boundary layer, leading-edge pressure distributions can be correlated if the vertical distance from the fin root Z is normalized by D. For small D/δ, the

correlation is still successful if the wall pressures are normalized using the local pitot pressure in the incoming boundary layer. For intermediate values of D/δ, when the shock wave structure is partially immersed in the boundary layer, the scaling is modified, but to first order, the primary scaling parameter is still D.

Although δ is not the appropriate parameter for correlating the length scales of the inner region of the interaction, the state of the incoming boundary layer is of critical importance. With a laminar layer, D still exerts a controlling influence, but the interaction scale in terms of it is increased significantly. Tests at Mach 5.3 show that centerline upstream influence is 9-12 D with a laminar layer, compared to 2-3D in the turbulent case. Two other parameters that also have large effects on the interaction scale are leading-edge sweepback angle and leading-edge shape. For hemicylindrically blunted leading edges, increasing the sweepback angle results in a rapid decrease in centerline upstream influence. The effects on spanwise development are not well documented, and a proper knowledge of them must await further study. As far as is known, no systematic studies have been made of the effects of leading-edge shape. The few existing results using flat leading edges show that the centerline upstream influence increases significantly compared with the hemicylindrically blunted case.

Acknowledgments

The experimental studies described here were supported by the Department of the Navy, Naval Air Systems Command, Contracts N60921-78-C-0068 and N60921-81-K-0007, monitored by Mr. W. Volz and Mr. D. Hutchins, and the U.S. Army Research Office, Grant DAAG29-77-G-0234, monitored by Dr. R. Singleton.

References

[1]Horstman, C.C. and Hung, C.M., "Computation of Three-Dimensional Turbulent Separated Flows at Supersonic Speeds," AIAA Paper 79-0002, Jan. 1979.

[2]Hung, C.M. and MacCormack, R.W., "Numerical Solution of Three-Dimensional Shock Wave and Turbulent Boundary Layer," AIAA Paper 78-161, Jan. 1978.

[3]Shang, J.S. and Hankey, W.L., "Numerical Solution of Compressible Navier-Stokes Equations for a Three-Dimensional Corner," AIAA Paper 77-169, Jan. 1977.

[4]Dolling, D.S. and Bogdonoff, S.M., "Scaling of Interactions of Cylinders with Supersonic Turbulent Boundary Layers," *AIAA Journal*, Vol. 19, May 1981, pp. 655-657.

[5]Sedney, R., "A Survey of the Effects of Small Protuberances on Boundary Layer Flows," *AIAA Journal*, Vol. 11, June 1973, pp. 782-792.

[6]Korkegi, R.H., "Survey of Viscous Interaction Associated with High Mach Number Flight," *AIAA Journal*, Vol. 9, May 1971, pp. 771-784.

[7]Cosad, C.D., "An Analysis of Blunt Fin Induced Shock Wave-Turbulent Boundary Layer Interactions," M.S.E. Thesis (1384-T), Dept. of Mechanical and Aerospace Engineering, Princeton Univ., Princeton, N.J., July 1978.

[8]Sedney, R. and Kitchens, C.W. Jr., "Separation Ahead of Protuberances in Supersonic Turbulent Boundary Layers," *AIAA Journal*, Vol. 15, April 1977, pp. 546-552.

[9]Voitenko, D.M., Zubkov, A.I., and Panov, Y.A., "Supersonic Gas Flow Past a Cylindrical Obstacle on a Plate," *Mekhanika Zhidkosti i Gaza*, Vol. 1, Jan.-Feb. 1966, pp. 121-125.

[10]Price, A.E. and Stallings, R.L., "Investigation of Turbulent Separated Flows in the Vicinity of Fin Type Protuberances at Supersonic Mach Numbers," NASA TN D-3804, Feb. 1967.

[11]Voitenko, D.M., Zubkov, A.I., and Panov, Yu A., "Influence of Mach Number on Flow in a Three-Dimensional Separation Region," *Moscow University Bulletin*, Ser. I, Mathematics and Mechanics, Vol. 23, No. 2, 1968, pp. 115-118.

[12]Uselton, J.C., "Fin Shock-Boundary Layer Interaction Tests on a Flat Plate with Blunted Fins at $M=3$ and 5," AEDC-TR-67-113, June 1967.

[13]Westkaemper, J.C., "Turbulent Boundary Layer Separation Ahead of Cylinders," *AIAA Journal*, Vol. 6, July 1968, pp. 1352-1355.

[14]Lucas, E.J., "Investigation of Blunt Fin-Induced Flow Separation Region on a Flat Plate at Mach Numbers 2.5 to 4.0," AEDC-TR-70-265, Jan. 1971.

[15]Kaufman, L.G., Korkegi, R.H., and Morton, L.C., "Shock Impingement Caused by Boundary Layer Separation Ahead of Blunt Fins," Aeronautical Research Lab., ARL 72-0118, Aug. 1972.

[16]Dolling, D.S., Cosad, C.D., and Bogdonoff, S.M., "Three-Dimensional Shock Wave Turbulent Boundary Layer Interactions—A Parametric Study of Blunt Fin-Induced Flows," AIAA Paper 78-159, Jan. 1978.

[17]Dolling, D.S., Cosad, C.D., and Bogdonoff, S.M., "An Examination of Blunt Fin-Induced Shock Wave Turbulent Boundary Layer Interactions," AIAA Paper 79-0068, Jan. 1979.

[18]Winkelmann, A.E., "Experimental Investigations of a Fin Protuberance Partially Immersed in a Turbulent Boundary Layer at Mach 5," (Naval Ordnance Lab.) NOLTR-72-33, 1972.

[19]Gillerlain, J.D., "Fin-Cone Interference Flowfield," AIAA Paper 79-0200, Jan. 1979.

[20]Dolling, D.S., "Comparison of Sharp and Blunt Fin-Induced Shock Wave Turbulent Boundary Layer Interaction," *AIAA Journal*, Vol. 20, Oct. 1982, pp. 1385-1391.

[21]Degrez, G., "Exploratory Experimental Investigation of the Unsteady Aspects of Blunt Fin-Induced Shock Wave Turbulent Boundary Layer Interactions," M.S.E. Thesis (1516-T), Dept. of Mechanical and Aerospace Engineering, Princeton Univ., Princeton, N.J., June 1981.

[22]Dolling, D.S. and Bogdonoff, S.M., "An Experimental Investigation of the Unsteady Behavior of Blunt Fin-Induced Shock Wave Turbulent Boundary Layer Interactions," AIAA Paper 81-1287, June 1981.

[23]Hung, F.T. and Clauss, J.M., "Three-Dimensional Protuberance Interference Heating in High Speed Flow," AIAA Paper 80-0289, Jan. 1980.

[24]Dolling, D.S. and Bogdonoff, S.M., "Experimental Investigation of Three-Dimensional Shock Wave Turbulent Boundary Layer Interaction—An Exploratory Study of Blunt Fin-Induced Flows," Princeton Univ., Princeton, N.J., M.A.E. Rept. 1468, March 1980.

[25]Dolling, D.S. and Bogdonoff, S.M., "Upstream Influence Scaling of Sharp Fin-Induced Shock Wave Turbulent Boundary Layer Interaction," AIAA Paper 81-0336, Jan. 1981.

[26]Edney, B., "Anomalous Heat Transfer and Pressure Distributions on Blunt Bodies at Hypersonic Speeds in the Presence of an Impinging Shock," Aeronautical Research Institute of Sweden, Stockholm, Sweden, Rept. 115, Feb. 1968.

[27]Tewfik, O.K. and Giedt, W.H., "Heat Transfer Recovery Factor and Pressure Distributions Around a Cylinder Normal to a Supersonic Rarefied Air Stream; Part I, Experimental Data," Univ. of California, Berkeley, Calif., Rept. HE-150-162, Jan. 1959.

[28]Miller, W.H., "Pressure Distributions on Single and Tandem Cylinders Mounted on a Flat Plate in Mach Number 5.0 Flow," Defense Research Lab., Univ. of Texas, Austin, Texas, DRL 538, June 1966.